# Kinematic Comparison of Pediatric Human Volunteers and the Hybrid III 6-Year-Old Anthropomorphic Test Device

Thomas Seacrist, Sriram Balasubramanian, J. Felipe García-España,
Matthew R. Maltese, Kristy B. Arbogast
Center for Injury Research and Prevention, The Children's Hospital of Philadelphia

Francisco J. Lopez-Valdes, Richard W. Kent
Center for Applied Biomechanics, University of Virginia

Hiromasa Tanji, Kazuo Higuchi
TK Holdings

**ABSTRACT** – The Hybrid III 6-year-old ATD has been benchmarked against adult-scaled component level tests but the lack of biomechanical data hinders the effectiveness of the procedures used to scale the adult data to the child. Whole body kinematic validation of the pediatric ATD through limited comparison to post mortem human subjects (PMHS) of similar age and size has revealed key differences attributed to the rigidity of the thoracic spine. As restraint systems continue to advance, they may become more effective at limiting peak loads applied to occupants, leading to lower impact environments for which the biofidelity of the ATD is not well established. Consequently, there is a growing need to further enhance the assessment of the pediatric ATD by evaluating its biofidelity at lower crash speeds. To this end, this study compared the kinematic response of the Hybrid III 6 year old ATD against size-matched male pediatric volunteers (PVs) (6-9 yrs) in low-speed frontal sled tests. A 3-D near-infrared target tracking system quantified the position of markers at seven locations on the ATD and PVs (head top, opisthocranion, nasion, external auditory meatus, C4, T1, and pelvis). Angular velocity of the head, seat belt forces, and reaction forces on the seat pan and foot rest were also measured. The ATD exhibited significantly greater shoulder and lap belt, foot rest, and seat pan normal reaction loads compared to the PVs. Contrarily, PVs exhibited significantly greater seat pan shear. The ATD experienced significantly greater head angular velocity (11.4 ± 1.7 rad/s vs. 8.1 ± 1.4 rad/s), resulting in a quicker time to maximum head rotation (280.4 ± 2.5 ms vs 334.2 ± 21.7 ms). The ATD exhibited significantly less forward excursions of the nasion (171.7 ± 7.8 mm vs. 199.5 ± 12.3 mm), external auditory meatus (194.5 ± 11.8 mm vs. 205.7 ± 10.3 mm), C4 (127.0 ± 5.2 mm vs. 183.3 ± 12.8 mm) and T1 (111.1 ± 6.5 mm vs. 153.8 ± 10.5 mm) compared to the PVs. These analyses provide insight into aspects of ATD biofidelity in low-speed crash environments.

## INTRODUCTION

Traumatic head injuries are the most common serious injury sustained by children in car crashes (Arbogast et al. 2005; Arbogast et al. 2002; Durbin et al. 2003; Howard et al. 2003; Orzechowski et al. 2003; Arbogast et al., 2004). Head injuries also account for one-third of all pediatric related injury deaths (Adekoya et al. 2002; Thompson and Irby 2003). Prevention of these injuries through effective motor vehicle safety systems is enhanced through the use of a biofidelic anthropomorphic test device (ATD) to ensure safety systems mitigate injuries in real children.

The Hybrid III 6-year-old ATD has been benchmarked at a component level (McPherson and Kriewall, 1981; Hubbard RP 1971; Hodgson et al. 1971; Foster et al. 1977; Viano et al. 1978; Haut et al. 1980) against response corridors that have been scaled from adult biomechanical data to account for geometric differences between adults and children (Irwin and Mertz 1997). Often these scaling efforts were hindered by lack of appropriate biomechanical data to adequately account for age-based material differences. Whole-body (i.e., system level) response requirements are under development (Shaw et al. 2009), but currently are not used in the design, assessment, or calibration of ATDs (pediatric or adult).

There have been limited efforts to validate the pediatric ATD in moderate to high speed loading (29-49 km/hr) against post mortem human subjects (PMHS) of similar size or age. (Sherwood et al. 2002; Lopez-Valdes et al. 2009) Results showed that, while peak displacements for the PMHS and ATD were similar, head rotation, thoracic spine flexion, and neck moments (Sherwood et al. 2002) as well as peak head and spine accelerations and torso angle (Lopez-Valdes et al. 2009) differed from the volunteers. The authors hypothesized that the rigid

ATD thoracic spine was a major contributor to the differences.

Future restraint systems, however may lead to an even greater diversity of loading environments as restraint designers attempt to limit crash loads and accelerations transmitted to the occupant. In fact, as restraints become more effective at limiting peak loads applied to occupants, it may become increasingly important to evaluate ATD biofidelity in loading environments that have historically been considered relatively benign. Consequently, there is a growing need to evaluate the biofidelity of the ATD in lower speed crash environments.

Biofidelic evaluation at lower speeds provides the ability to compare the ATD to the kinematics of human volunteers. Low to moderate impact frontal sled tests have been performed using adult volunteers (18+ yrs) to establish and evaluate ATD performance. Using data from the Naval Biodynamics Laboratory (NBDL), Wismans et al (1986) measured the kinematic and load response of the adult head and neck to establish omni-directional biofidelity requirements for the ATD neck at moderate severity (6-16 g's). Begeman et al (1980) compared relaxed and tensed adult volunteer responses to $-G_x$ acceleration (6.2g max) to a PMHS and the Part 572 ATD. Results showed that, while the PMHS and ATD were similar in nature, restraint loads and dynamic response differed substantially from both surrogates, with the PMHS and ATD falling between the relaxed and tensed responses of the humans.

Recently, Arbogast et al (2009) compared the kinematic responses and restraint loads of pediatric volunteers (6-14 yrs) with adults (18-30 yrs) in low speed frontal crash conditions (< 4 g). These data represent a valuable dataset to which to compare the kinematics response of the Hybrid III 6 year old ATD. To this end, the current study compares the kinematic response of the Hybrid III 6 year old ATD to size-matched pediatric volunteers (PVs) in low speed frontal crash conditions. These analyses begin to quantify the biofidelity of the ATD outside of regulatory conditions and provide insight into aspects of ATD biofidelity in low-speed crash environments.

## METHODS

This study protocol was reviewed and approved by the Institutional Review Boards at The Children's Hospital of Philadelphia, Philadelphia, PA and Rowan University, Glassboro, NJ.

**Table 1. Anthropometric Measures**

| Subject | Age (yr) | Mass (kg) | Erect Seated Height (cm) | ESSH (cm) |
|---|---|---|---|---|
| HIII | 6 | 23.4 | 63.5 | 64.1 ± 0.1 |
| PV1 | 6 | 24.1 | 69.0 | 63.6 ± 0.9 |
| PV2 | 7 | 23.6 | 66.0 | 61.9 ± 1.1 |
| PV3 | 9 | 25.2 | 65.5 | 60.5 ± 0.9 |

### Pediatric Volunteers

Of 20 PVs tested (Arbogast 2009), three were selected for comparison with the Hybrid III 6 year old ATD. Specific inclusion criteria were pediatric subjects whose erect seated height and mass were within ± 10% of the ATD (63.5 cm, 23.4 kg). Key anthropometric measures for the subjects and ATD are listed in Table 1. An environment-specific seated height (ESSH) was measured as the z-axis (vertical) height of the head top marker with the subject in his initial position. Mass (PV 95% CI: 22.9 – 25.7 kg), and ESSH (PV 95% CI: 59.3 – 64.7 cm) were not significantly different between the ATD and PVs. Informed consent was obtained from a parent or guardian and informed assent from the pediatric volunteers.

### Instrumentation and Testing

A comprehensive description the testing method can be found in Arbogast et al (2009). Briefly, healthy male pediatric subjects between ages 6 to 14 years whose height, weight, and body mass index (BMI) were within 5th and 95th percentile for the subject's age were recruited.

Subjects were seated in a pneumatically actuated, hydraulically controlled low acceleration sled. A safe, non-injurious crash pulse applicable to the pediatric population was derived from an amusement park bumper car impact. The volunteer sled was equipped with an onboard accelerometer and two six axis load cells placed under the seat pan and foot rest.

Subjects were restrained using an automotive three-point belt system (Takata Corp., Tokyo, Japan) consisting of commercially available components including an emergency locking retractor (locking threshold: 2g) with automatic locking retractor function, webbing with 10-12% elongation, and cinching latch. Lightweight belt webbing load cells (Model 6200FL-41-30, Denton ATD Inc, Rochester Hills, MI) were attached five inches from the D-ring location on the shoulder belt between the subject and the D-ring and on the right and left locations on the lap belt.

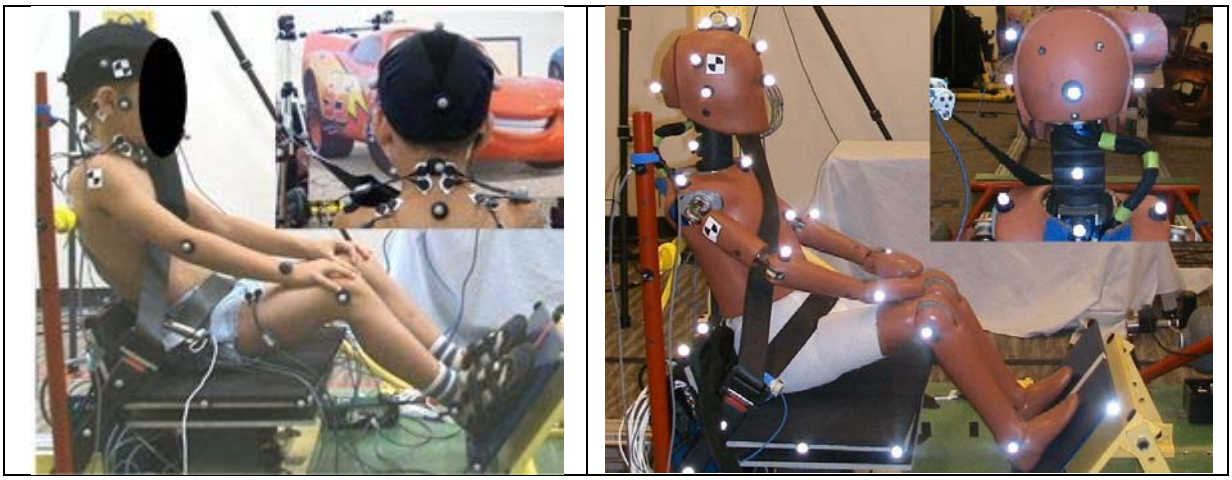

**Figure 1.** Instrumentation and initial position comparison of a PV (left) and ATD (right).

Photoreflective markers were placed on anatomical landmarks of interest including the head top (HT), opisthocranion (OP), nasion (NAS), external auditory meatus bilaterally (EAM), C4, T1, and the left iliac crest and were tracked using a 3D motion analysis system (Model Eagle 4 Motion Analysis Corporation, Santa Rosa, CA). An angular rate sensor (ARS-300, DTS Inc, Seal Beach, CA) was mounted via a custom fixture to a subject-specific athletic mouth guard to measure the head rotational speed.

The initial position of the torso and knee angles were set to 110° by adjusting the fore-aft position of the footrest and vertical position and tightness of the nylon strap backrest to mimic the posture of a rear seated occupant in an automobile (Reed et al. 2005). The height of the shoulder belt anchor was adjusted to provide similar fit across subjects; specifically, the shoulder belt angle at the D-Ring (defined as the angle the shoulder belt makes with the horizontal) was set at 70º at initial position for all the subjects. The lap belt anchor locations were fixed throughout the test series and the lap belt buckle angle (defined as the angle the lap belt buckle makes with the horizontal) was set at 70 degrees at initial position for all the subjects. Knee/torso angle and seat belt angle were established using a goniometer and inclinometer, respectively. A single technician oriented all human volunteers and the ATD, eliminating inter-technician variability. PVs were oriented immediately prior (<10 sec) to triggering the sled, thus minimizing the time for subjects to deviate from initial position. Variation in human volunteer initial position was previously shown not to be a significant factor influencing trajectories for this data set (Arbogast 2009). To minimize the effect of initial head angle, subjects were asked to position their head by focusing on a point placed directly in front of them at the level of their nasion. A detailed analysis of initial position for individual subjects and markers can be found in Arbogast et al. (2009).

Pediatric volunteers received six consecutive, repeated trials with approximately 10 minutes between trials. ATD marker placement and initial position mimicked the methodology used for the pediatric subjects (Figure 1). Three repeated trials were performed using the Hybrid III 6 year old ATD.

**Data Acquisition and Processing**

Signals from the ARS, accelerometer and load cells were sampled at 10,000 Hz using a T-DAS data acquisition system (Diversified Technical Systems Inc., Seal Beach, CA) with a built-in anti-aliasing filter (4,300 Hz). The sled acceleration data, seat belt loads, and forces and moments at the seat pan and foot rest were filtered at SAE channel frequency class (CFC) 60, as recommended by the SAE J211 recommended practice (Society of Automotive Engineers 1995). The ARS signal was filtered at CFC 1000. The Motion Analysis data were acquired at 100 Hz and analyzed using EVaRT5 software (Motion Analysis Corporation, Santa Rosa, CA).

**Data Reduction**

The time series motion analysis and T-DAS data were imported into MATLAB (Mathworks, Inc., Natick, MA) for data analysis using a custom written program. The primary outcomes of interest were trajectories of the head, upper neck, and pelvis as well as reaction forces of the foot rest, seat belt, and seat pan. The marker at the right rear of the seat pan was designated as the origin for the local (sled) coordinate system. All trajectories were projected onto the sagittal plane. Delta excursions were computed in the x and z direction as the change from

**Table 2. Reaction Loads**

| | ATD (N) | PVs (N) | PV 95% CI (N) |
|---|---|---|---|
| SB* | 338 ± 58 | 190 ± 47 | 121 – 260 |
| LBL* | 452 ± 67 | 123 ± 51 | 99 – 148 |
| LBR* | 508 ± 73 | 130 ± 52 | 93 – 168 |
| SPX* | 1756 ± 151 | 2871 ± 248 | 2396 – 3346 |
| SPZ* | 2784 ± 510 | 1474 ± 601 | 2396 – 3346 |
| FRX* | 668 ± 77 | 355 ± 58 | 250 – 461 |
| FRZ* | 1980 ± 179 | 1481 ± 164 | 1305 – 1656 |

* indicates significant differences at the 0.05 level

initial position to maximum excursion. Time of max x and z excursion were computed for HT, C4, and T1. Out-of-plane movement was calculated for the aforementioned markers of interest as the y-component at maximum forward head excursion expressed as a percentage of resultant excursion (Arbogast et al. 2009). Average trajectories, excursions, acceleration, head rotation, and loads across trial and subject were computed for the pediatric volunteer group and compared to the ATD.

### Statistical Analysis

Data were imported into SUDAAN 10.0 (Research Triangle Institute, Research Triangle Park, NC) for statistical analysis, and analyzed using both descriptive and inferential statistical techniques. Analysis occurred in three distinct phases. In phase I, descriptive statistics such as frequency distributions, histograms and measures of central tendency, variability, and association were computed for all relevant variables in the dataset. In order to use appropriate statistical methods, variables were tested for normality. In phase II, bivariate plots were generated in which head and neck trajectories were plotted for each subject and the ATD. In phase III, inferential statistical techniques were applied. To account for clustering of trials according to pediatric volunteer, robust variances were computed by using Taylor series linearization method and 95% CI were estimated for all parameters. Differences - in weight, seated height, delta v, maximum delta excursions, maximum forces, ARS velocity, ARS angle, etc.- between the ATD and the PVs were assessed by comparing the ATD's mean value to the corresponding PVs 95% CI. The experiment wise error rate was held at the 0.05 level.

**Table 3. Head Angular Velocity and Rotation**

| | ATD | PVs | PV 95% CI |
|---|---|---|---|
| Rotation (°) | 47.0 ± 3.7 | 39.8 ± 5.5 | 30.7 – 48.9 |
| Time (ms)* | 280.4 ± 2.5 | 334.2 ± 21.7 | 310 – 360 |
| Vel. (rad/s)* | 11.4 ± 1.7 | 8.1 ± 1.4 | 6.5 – 9.6 |
| Time (ms)* | 246.2 ± 2.2 | 256.3 ± 6.4 | 250 – 260 |

* indicates significant differences at the 0.05 level

## RESULTS

### Acceleration Pulse and Delta V

The acceleration pulse from all trials, all PVs were averaged and plotted in Figure 2. The ATD experienced slightly higher peak acceleration (4.08 ± 0.34 g in 61.7 ± 1.1 ms; Duration: 120.1 ± 2.0 ms) than the PVs (3.60 ± 0.15 g in 55.3 ± 16.6 ms; Duration: 128.1 ± 2.5 ms). However, the ATD (2.46 ± 0.1 m/s) and PVs (2.47 ± 0.05 m/s) exhibited nearly identical delta v, with an average difference of 0.3%. Delta v was calculated as the change in velocity of the sled at the time point when shoulder belt loads return to 5% of their maximum value.

### Seat Belt, Seat Pan, and Foot Rest Loads

Time histories for the shoulder belt (SB) and left lap belt (LBL) for the PVs and the ATD (all trials, all subjects plus average) are shown in Figures 3-4. Time histories of the seat pan shear (SPX) and normal (SPZ) load are shown in Figures 5-6. Time histories of the foot rest shear (FRX) and normal (FRZ) load are shown in Figures 7-8. Mean (±SD) peak load are listed in Table 2.

### Angular Velocity and Head Rotation

Time histories of the change in head angle and angular rate are shown in Figures 9-10. Mean (±SD) peak and time of peak are listed in Table 3.

### Trajectories and Excursions

Significant reductions in ΔX excursion were observed in the ATD for the NAS, EAM, C4 and T1 (Table 4) and ΔZ excursion for the C4, T1, and pelvis (Table 5). These differences were accompanied by significantly quicker time to peak ΔX and ΔZ in the ATD as well as significant delays between ΔX and ΔZ for the PVs' HT (Table 6). Peak change in knee angle did not differ between the ATD (24.1° ± 1.1°) and the PVs (22.7° ± 3.4°). Raw trajectories relative to the cart (Figure 11) and relative to T1 (Figure 12) are shown.

**Table 4. ΔX-Excursion**

| Marker | ATD (mm) | PVs (mm) | PV 95% CI (mm) |
|---|---|---|---|
| HT | 271.8 ± 16.4 | 295.0 ± 21.0 | 263.4 – 326.7 |
| OP | 216.4 ± 12.3 | 246.5 ± 22.0 | 207.8 – 285.2 |
| NAS* | 171.7 ± 7.8 | 199.5 ± 12.3 | 192.2 – 206.9 |
| EAM* | 194.5 ± 11.8 | 205.7 ± 10.3 | 202.4 – 209.0 |
| C4* | 127.0 ± 5.2 | 183.3 ± 12.8 | 168.4 – 198.1 |
| T1* | 111.1 ± 6.5 | 153.8 ± 10.5 | 152.5 – 155.1 |
| Pelvis | 78.3 ± 1.5 | 78.7 ± 16.4 | 51.1 – 106.3 |

* indicates significant differences at the 0.05 level

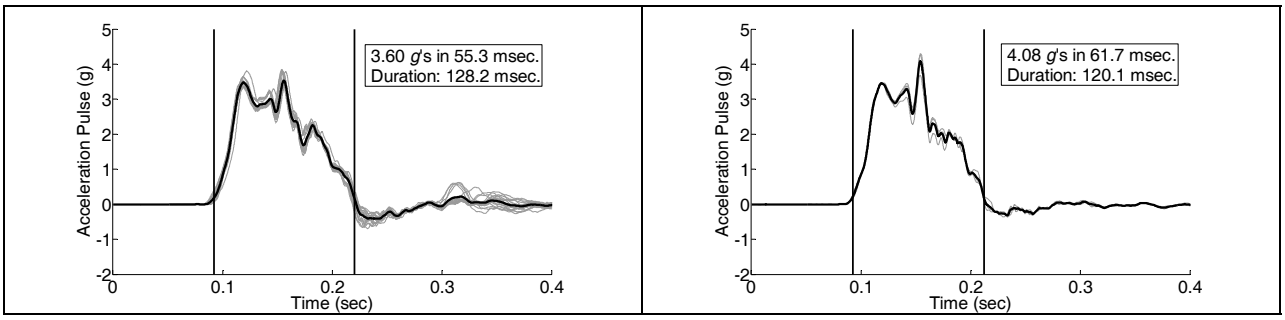


**Figure 2.** Average sled acceleration pulse with peak values for PVs (left) and ATD (right). The gray lines indicate acceleration pulse for each trial, each subject, whle the black line represents the average. Vertical lines indicate onset and end of sled acceleration pulse, defined as the time at which acceleration reaches 5% of its maximum value.

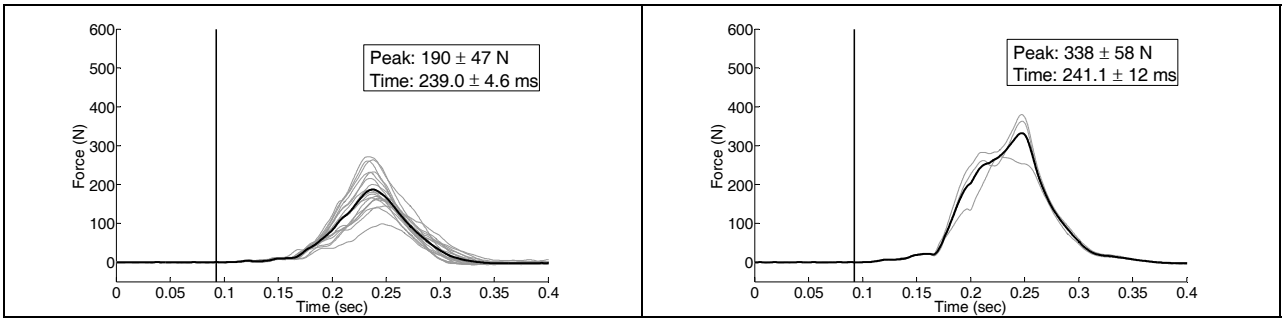


**Figure 3.** Time history of the shoulder belt loads for PVs (left) and ATD (right). Vertical line indicates the onset of sled acceleration. Peak and time of peak (Mean ± SD) are listed.

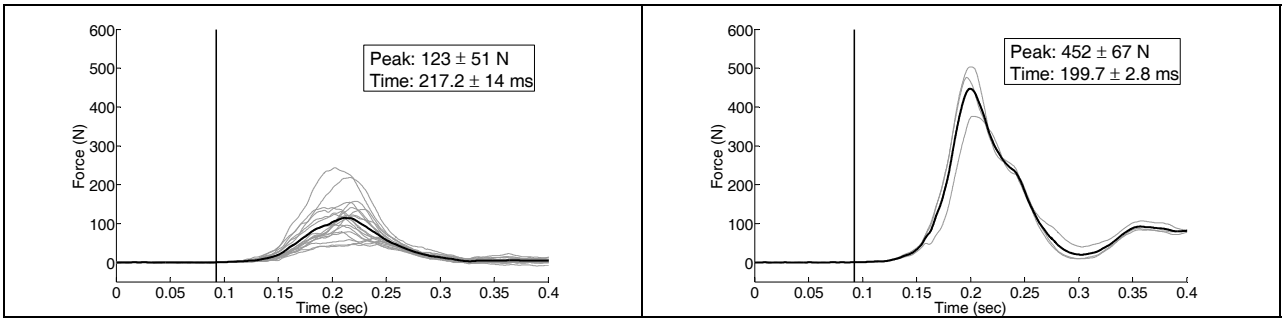


**Figure 4.** Time history of the lap belt loads (left) for PVs (left) and ATD (right). Vertical line indicates the onset of sled acceleration. Peak and time of peak (Mean ± SD) are listed.

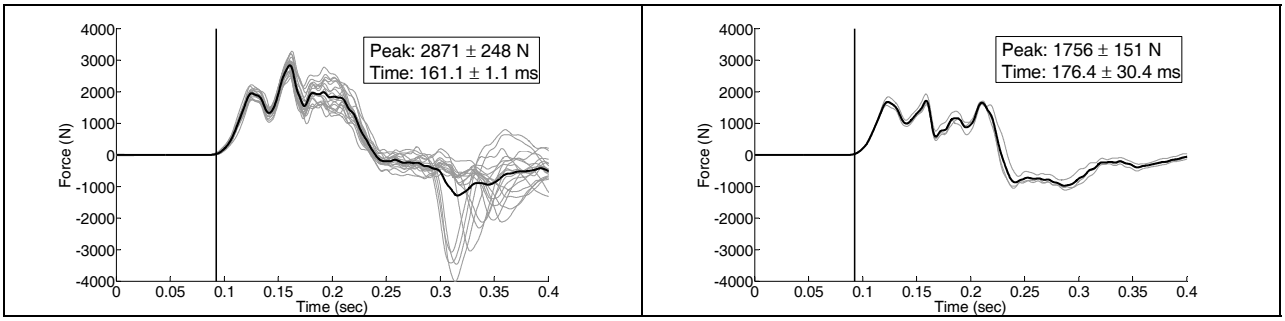


**Figure 5.** Time history of the seat pan shear (x-axis) load for PVs (left) and ATD (right). Vertical line indicates the onset of sled acceleration. Peak and time of peak (Mean ± SD) are listed.

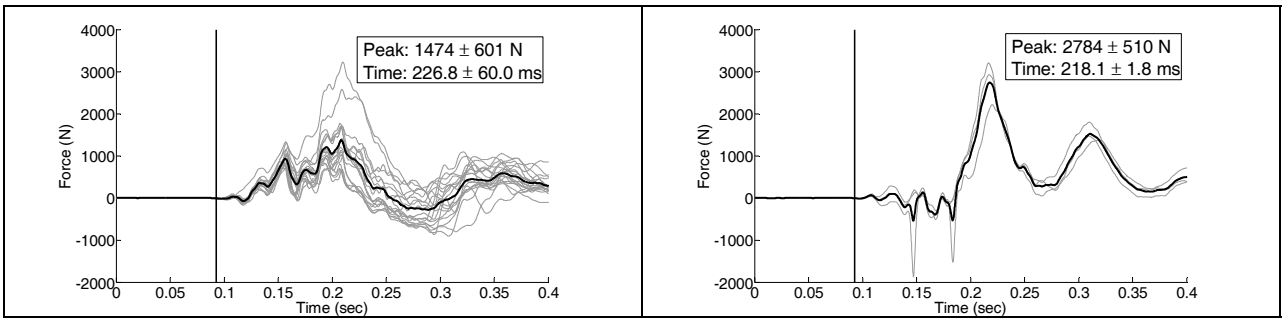


**Figure 6.** Time history of seat pan normal (z-axis) load for PVs (left) and ATD (right). Vertical line indicates the onset of sled acceleration. Peak and time of peak (Mean ± SD) are listed.

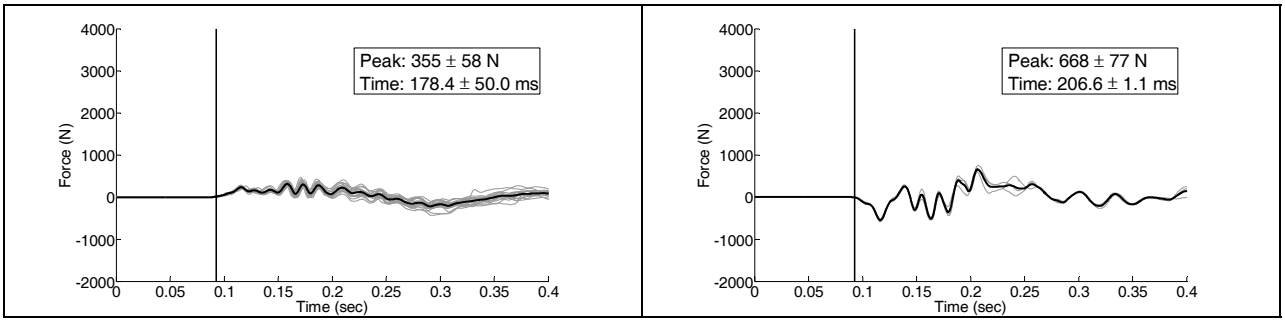


**Figure 7.** Time history of foot rest shear (x-axis) load for PVs (left) and ATD (right). Vertical line indicates the onset of sled acceleration. Peak and time of peak (Mean ± SD) are listed.

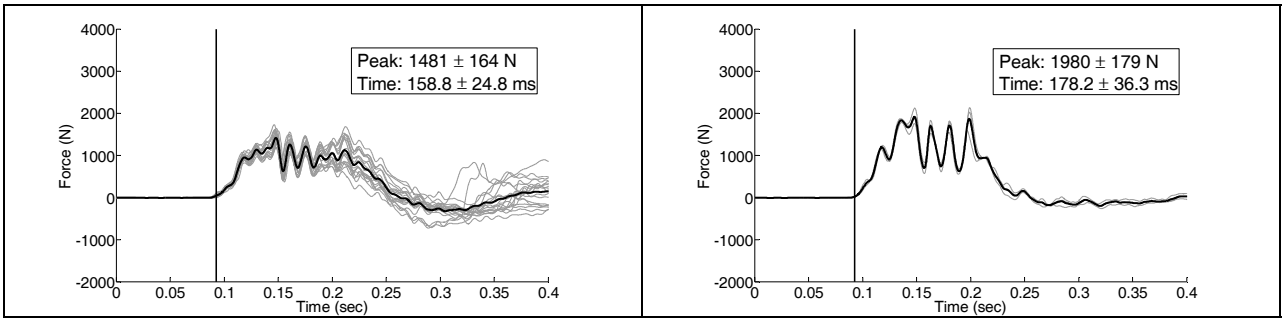


**Figure 8.** Time history of foot rest normal (z-axis) load for PVs (left) and ATD (right). Vertical line indicates the onset of sled acceleration. Peak and time of peak (Mean ± SD) are listed.

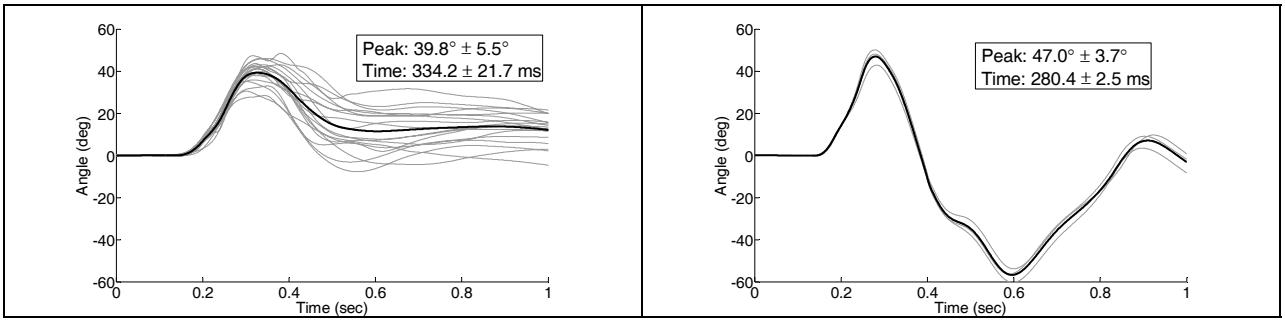


**Figure 9.** Time history of the change in head angle for PVs (left) and ATD (right). Vertical line indicates the onset of sled acceleration. Peak and time of peak (Mean ± SD) are listed.

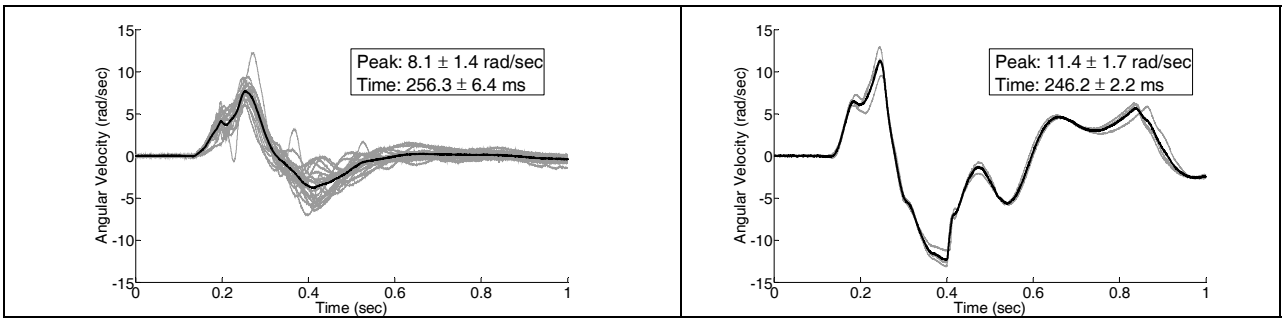


**Figure 10.** Time history of the head angular velocity for PVs (left) and ATD (right). Vertical line indicates the onset of sled acceleration. Peak and time of peak (Mean ± SD) are listed.

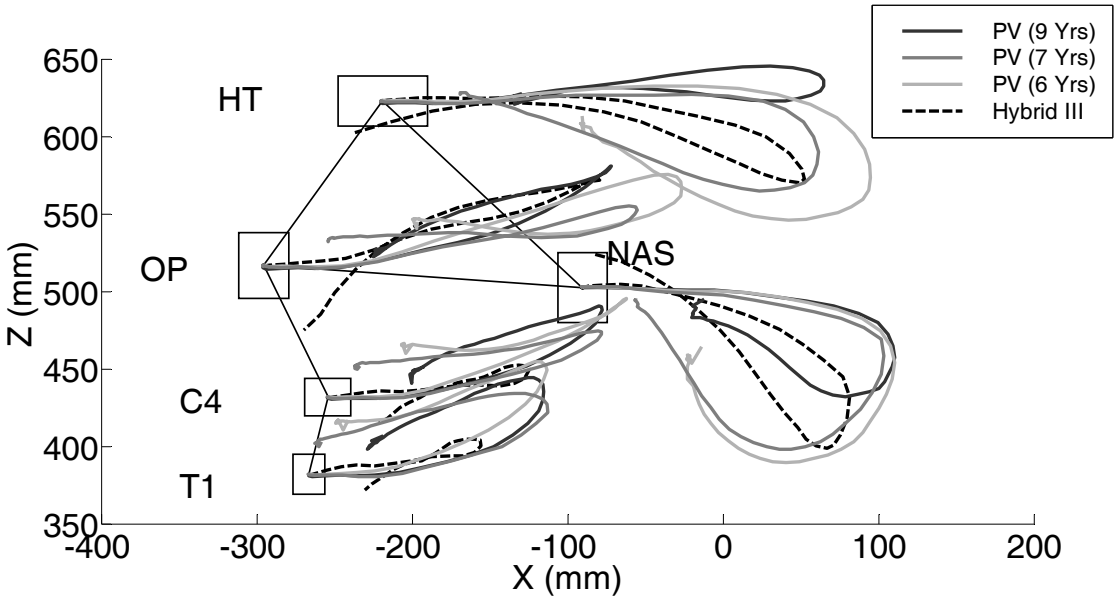


**Figure 11.** Head and neck trajectories in the sagittal plane. Trajectories are aligned with the average initial position of each marker. Rectangles represent one standard deviation of marker initial position.

**Table 5. ΔZ-Excursion**

| Marker | ATD (mm) | PVs (mm) | 95% CI (mm) |
|---|---|---|---|
| HT | -52.7 ± 1.9 | -49.4 ± 31.7 | -106.5 – 7.7 |
| OP | 55.9 ± 7.0 | 54.7 ± 16.0 | 30.1 – 79.2 |
| NAS | -103.9 ± 6.6 | -96.2 ± 24.8 | 135.0 – -57.4 |
| EAM | -39.4 ± 1.9 | -38.6 ± 15.2 | -61.7 – -15.5 |
| C4* | 16.3 ± 7.4 | 55.9 ± 13.1 | 36.6 – 75.2 |
| T1* | 22.7 ± 5.1 | 63.4 ± 12.1 | 46.1 – 80.6 |
| Pelvis* | -8.8 ± 1.8 | 22.4 ± 7.6 | 12.9 – 32.0 |

* indicates significant differences at the 0.05 level. Negative z excursion indicates movement downward.

**Table 6. Time of Max Excursion**

| | Marker | ATD (ms) | PV (ms) | PV 95% CI (ms) |
|---|---|---|---|---|
| ΔX | HT* | 280 ± 10 | 300 ± 10 | 290 – 320 |
| | C4 | 250 ± 10 | 280 ± 20 | 250 – 320 |
| | T1 | 250 ± 10 | 270 ± 20 | 250 – 290 |
| ΔZ | HT* | 290 ± 0 | 360 ± 90 | 330 – 390 |
| | C4* | 260 ± 20 | 290 ± 10 | 290 – 300 |
| | T1* | 260 ± 0 | 300 ± 20 | 300 – 310 |
| ΔX – ΔZ | HT* | -10 ± 10 | -50 ± 90 | -80 – -30 |
| | C4 | -20 ± 30 | -10 ± 20 | -40 – 20 |
| | T1 | -10 ± 10 | -30 ± 20 | -50 – -10 |

* indicates significant differences at the 0.05 level.

## DISCUSSION

This study sought to evaluate the biofidelity of the Hybrid III 6 year old ATD in low speed frontal crash tests by comparing its response to that of pediatric volunteers in similar loading environments. This effort represents the first effort to directly compare whole body kinematics of the pediatric ATD to living children. The results highlighted differences in reaction forces and head and spine kinematics between the ATD and children that may influence how an actual child interfaces with a restraint system and moves during automotive-like loading.

### Test Environment and Initial Position

In order to visualize the markers along the spine, the current test setup did not use a full backrest. Instead, an adjustable nylon strap was used as a back support to provide minimal support for the subjects' torso in the initial position. A standard 3 point seat belt was adjusted to the height of the ATD and PVs. The setup was not designed to mimic any specific automobile but rather to provide an automotive-like posture in which to compare the ATD and human. Interestingly, while whole body initial position was similar between the ATD and PVs (110º knee and torso angle), body segment posture differences were observed between the ATD and PVs (Figure 1). The PVs achieved a 110º torso angle with a more slumped posture than the ATD due to the additional degrees of freedom of the segmented human thoracic and lumbar spine. The contribution of these body segment posture differences to the overall kinematics described herein is unknown.

### Reaction Forces

The results highlight large differences in restraint loading, with the ATD exhibiting shoulder belt loads approximately 2x greater and lap belt loads approximately 4x greater than the PVs. One of the primary differences between the ATD and the PVs is the presence of active muscle response and potential awareness of the event. This is evidenced by intra-subject scatter of the PV reaction loads which is likely due to inherent variability in involuntary muscle activity during the event. Variations in muscle activity (voluntary or involuntary) may affect the interaction between the human volunteer and the restraint system/seating environment, producing variations in peak reaction forces. Of note, the ATD exhibited average shoulder and lap belt loads that were 25% and 107% greater than the maximum load experienced by any PV.

Previous work comparing relaxed and tensed adult volunteers during low speed impacts indicated that, while reflex response does not produce significant changes to occupant accelerations or restraint loading, pre-impact bracing of the lower limbs could significantly reduce accelerations and restraint loads (Begeman et al. 1980). If the reduction of restraint loads in the PVs was due to pre-impact bracing with the lower limbs, one would expect the PVs to exhibit increased foot rest load. However, the current study observed an opposing trend: the ATD exhibiting increased foot rest shear and normal load. Obviously, the ATD is incapable of producing a tensed muscle response. However, it is possible that the hip, knee, and ankle joints of the ATD are stiffer than the PVs, particularly since the ATD is designed to mimic lower extremity motion for high speed impacts. Increased rigidity of the lower extremities results in increased load being transferred to the footrest (Begeman et al, 1980). Another possible explanation is that, while PVs and the ATD were matched based on overall mass, the segment mass of the lower limbs may have differed. If the ATD lower extremities weighed more than the PVs, the increase in foot rest loads could simply be the result of a difference in inertial loading.

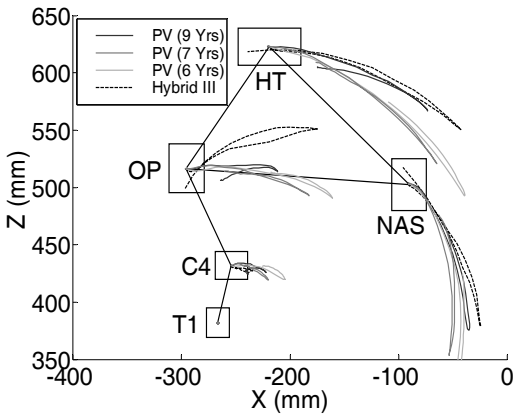


**Figure 12.** Head and neck trajectories in the sagittal plane relative to T1. Trajectories are aligned with the average initial position of each marker. Rectangles represent the one standard deviation of marker initial position.

Similar trends in reaction loads have been observed in a low speed comparison of the Hybrid III 50$^{th}$ male ATD and an adult PMHS, both of which are not subject to awareness or pre-impact bracing (Lopez-Valdes et al. in review AAAM 2010). In their study, greater shoulder belt and lap belt loads were observed in the ATD while the PMHS exhibited greater seat pan shear. Additionally, both the relaxed and tensed adult volunteers from Begeman et al (1980) exhibited reduced shoulder belt load, increased seat shear, and increased pelvis

acceleration compared to the ATD. These data suggest that the differences observed in the current study are not solely due to awareness or muscle response. Rather, they result from differences between the interaction of the ATD and PMHS/PV with the restraint system and seating environment. While the ATD is primarily restrained by the shoulder and lap belt, a larger portion of the PV load is being absorbed through seat pan shear. This result may be due to differences in the interaction of human tissue and clothing with the seat pan compared to the artificial exterior surface of the ATD, which is not necessarily designed to mimic response of the skin subjected to shear force at low speeds. Attempts were made to mimic the clothing worn by the subjects on the ATD. Additionally, the fact that increased seat pan shear was observed in Lopez Valdez et al using a PMHS and ATD suggests that the difference is not solely an artifact of clothing worn during the test.

**Head and Spine Kinematics**

Similar to previous studies comparing the pediatric ATD to PMHS (Sherwood et al 2002; Lopez-Valdes 2009), these results show that the global forward excursion of the head top – the most relevant marker to assess total head excursion – does not significantly differ between the PVs and the ATD. However, the method by which the subject reaches maximum head excursion is different between the PVs and the ATD. The ATD achieved similar HT x-excursion to the PVs despite reduced x- and z-excursion of the C4 and T1. This finding suggests greater rotation or translation of the head relative to the upper neck of the ATD. Gross head rotation demonstrated a non-significant trend of greater rotation for the ATD (48°) compared to the PVs (40°). However, it is important to note that head rotation relative to the sled coordinate system results from a combination of cervical, thoracic, and pelvis rotation. The ATD may be exhibiting reduced thoracic flexion and, consequently, increased cervical flexion compared to the PVs due to the rigidity of the ATD thoracic spine. Differences in thoracic response of the ATD compared to PMHS and PVs has been noted in previous studies. Sherwood et al. (2002) illustrated limitations in the biofidelity of the thoracic spine by showing increased thoracic flexion of the PMHS compared to no thoracic flexion in the ATD. Furthermore, previous work (Arbogast et al. 2009), has shown that human volunteers (6-14 and 18-30 yrs) exhibited thoracic spine flexion in identical low-speed sled tests with the greatest flexion occurring in the 6-8 year old age range. To further explore this concept and examine differences between the ATD and PV above the thoracic spine, trajectories were also plotted with respect to the T1 marker (Figure 12). Differences in head trajectory between the ATD and PV were less apparent when examined relative to T1, further highlighting the contribution of the thoracic spine in the overall head kinematics of the human. However, even relative to T1, differences in trajectory are still observable. The ATD continued to exhibit reduced ΔZ excursion of the HT, OP, and NAS compared to the 6 and 7 year PVs. This suggests limitations in the biofidelity of the ATD cervical spine in low speeds. Interestingly, the 9 year old PV closely resembles the ATD in terms of HT, NAS, and OP trajectory shape (Figure 11). While the ATD does exhibit a difference in raw Z excursion compared to the 9 year old PV, the difference is likely the result of the lack of upward motion of the C4 and T1 marker in the ATD. When trajectories were aligned with T1 (Figure 12), the 9 year PV continued to resemble the ATD trajectories to an even greater degree, exhibiting reduced ΔZ of the HT and NAS relative to the younger PVs. Arbogast et al (2009) illustrated significant changes in head trajectory that occurred with age even after accounting for stature differences. Consequently, the 9 year PV may not be the best comparison to an ATD designed to represent a 6 year old.

Of note, reported differences in head and spine excursion were not due to differences in forward motion of the pelvis; increased x-excursion did not result from the PVs sliding further forward on the seat. A significant difference in ΔZ of the pelvis was detected; the pelvis marker moves upward in PVs, while the ATD exhibits downward motion. The upward motion is likely due to rearward pelvis motion as the subject becomes more upright (Arbogast et al. 2009). Differences in the anthropometry of the pediatric pelvis compared to the Hybrid III 6 year old have been illustrated in previous studies (Chamouard et al 1996; Reed et al 2009), specifically that the anterior-superior iliac spines (ASIS) are lower in the ATD compared to similar-size children (Chamouard et al 1996). This has important implications for lower restraint interaction, which require further study.

The ATD did exhibit significant rebound compared to the PVs. This is likely due to the absence of muscle response in the ATD. A meta-analysis of previous studies showed that the time required for muscle to produce significant reflex force to resist motion ranges from 150 – 200 ms from the onset of perturbation (Panjabi et al. 1998). This suggests that onset of reflex response in this study occurred from 240 – 290 ms (150 – 200 ms + 90 ms to onset of

sled acceleration), which is slightly prior to maximum HT x-excursion in the PVs. Thus, reflex response may have influenced the lack of rebound in the PVs. The ATD is not designed to simulate the active muscle response demonstrated by the PVs in low-speed frontal crashes. Further study is needed to determine if muscle response plays an important role at higher speeds and must be incorporated into the ATD design.

Of particular importance to injury assessment is the longer time to reach maximum head rotation, HT $\Delta X$ and HT $\Delta Z$ for the PVs. The additional 54 ms required to reach maximum forward flexion in the PVs may increase the likelihood of head contact injury especially in crashes in which intrusion into the occupant's seating position is critical to the injury causation. An ATD with its quicker time to max head excursion and substantial rebound may have its head away from the intruding structure whereas the PV's head may still be located where contact with the intruding structure is likely. It is important to note that, while this experiment compared the ATD and PVs in a pure frontal impact where intrusion into the rear occupant compartment is unlikely, real world crashes are rarely full frontal and may involve intrusion of structures such as the front seat back into a rear seated occupant's seating position due to the oblique nature of the crash. Further study is needed to determine if the more rapid head kinematics of the ATD observed at low speeds are demonstrated at higher crash speeds as well.

The observed increase in angular velocity may help explain previous observations that the Hybrid III 6 year old exceeded the neck injury criteria (Nij) during high speed tests (Menon et al. 2004; Menon et al. 2005). An increased angular velocity of the head may result in increased loads applied to the upper neck. This is supported by the finding that the ATD achieved similar HT excursion to the PVs despite reduced excursion of the C4 and T1. In order to exhibit identical head top excursion with reduced lower neck motion, the ATD upper neck may need to experience increased shear, tension, and/or moment. Further study is needed to compare the forces and moments of the ATD and PVs.

### Limitations

Several limitations of this study warrant discussion. First, marker trajectories were projected onto the x-z plane. Some out of plane motion did occur, but was approximately 3% for the PV and 10% for the ATD. The consequence of this projection is a slight under-reporting of total marker excursion. Additionally, the pediatric data herein was compared a single pediatric ATD. The Q-Series 6 Year Old ATD, for example, may exhibit different results. Finally, the ATD-PV differences were evaluated for a single crash condition. Results may differ in higher loading environments.

### Future Implications

These data provide a new data set to further optimize the ATD in low speed collisions. A logical next step is to use the current data as a validation dataset for a computational ATD or human body model or physical ATD. Once optimized to these new data, the model or ATD can be exercised in crash relevant scenarios to determine if the observed kinematic differences at low speed result in relevant differences between the kinematics of the current and modified ATD at higher speeds.

Whole body kinematics of a restrained occupant are governed by the interaction of a variety of different body components such as the thoracic and lumbar spines, abdomen, pelvis, and soft tissues. The specific contributions of these components to the whole body motion described herein are yet unknown and are an area of future study. While the results suggest increasing the flexibility of the thoracic spine may improve the kinematics of the ATD, optimization of the pediatric ATD to match human kinematics will likely require additional modifications including improvements to the rate-sensitivity of the abdomen (Rouhana et al 2001; Elhagediab 2007), abdominal anthropometrics (Elhagediab 2007) and pelvis shape (Reed et al 2009).

## CONCLUSION

In low-speed loading frontal crash conditions, the Hybrid III 6 year old ATD exhibited differences in excursion and reaction forces compared to similarly-sized pediatric volunteers (PV). The ATD exhibited significantly larger shoulder and lap belt, foot rest shear and normal, and seat pan normal reaction loads compared to the PVs. Contrarily, PVs exhibited significantly greater seat pan shear. The ATD experienced significantly larger head angular velocity resulting in a quicker time to maximum head rotation. The ATD exhibited significant reductions in nasion, EAM, C4 and T1 $\Delta X$ and $\Delta Z$ excursions. These results are not solely due to differences in the ATD cervical spine response and may be attributed, in part, to the rigidity of the ATD thoracic spine. These analyses provide insight into aspects of ATD biofidelity in low-speed crash environments.

**ACKNOWLEDGMENTS**

The authors would like to thank all the human volunteers who participated in this study for their patience and willingness to take part in this research. The authors would like to thank Mike Beebe of Denton ATD, Inc. for use of the Hybrid III 6 Year Old ATD. The authors would like to acknowledge Takata Corporation, Japan for their collaboration and financial support for this study. The results presented in this report are the interpretation solely of the author(s) and are not necessarily the views of Takata Corporation.

**REFERENCES**

Adekoya N, Thurman D, White D, Webb K. Surveillance for traumatic brain injury deaths – United States. MMWR Surveill Summ Vol. 51, No. 10, pp 1-14, 2002.

Arbogast KB, Corejo RA, Kallan MJ, Winston FK, Durbin DR. Injries to children in forward-facing child restraint systems in side impact crashes. Ann Proc Assoc Adv Automot Med Vol. 46, pp 213-230, 2002.

Arbogast KB, Chen I, Durbin D, Winston FK. Injury risks for children in child restraint systems in side impact crashes. Proc. International Research Conference on the Biomechanics of Impact Graz, Austria, 2004.

Arbogast KB, Jermakian JS, Ghati, Y, Smith R, Menon RA, Maltese MR. Patters and predicors of pediatric head injury. Proc. International Research Council on The Biomechanics of Impact Prague, Czech Republic, 2005.

Arbogast KB, Balasubramanian S, Seacrist T, Maltese MR, Garcia-Espana JF, Hopely T, Constans E, Lopez-Valdes FJ, Kent RW, Tanji H, Higuchi K. Comparison of Kinematic Responses of the Head and Spine for Children and Adults in Low-Speed Frontal Sled Tests. Stapp Car Crash Journal Vol. 53, pp 329-372, 2009.

Begeman PC, King AI, Levine RS, Viano DC. Biodynamic response of the musculoskeletal system to impact acceleration. SAE Paper No. 801312. In Proceedings of the 24th Stapp Car Crash Conference, Troy, MI, 1980.

Chamouard F, Tarriere C, Baudrit P. Protection of children on board vehicles: Influence of pelvis design and thigh and abdomen stiffness on the submarining risk for dummies installed on a booster. In: Proceedings of the 15th International Technical Conference on the Enhanced Safety of Vehicles. Paper Number 96-S7-O-03. National Highway Traffic Safety Administration, Washington, DC, 1996.

Durbin D, Elliot M, Winston F. Belt positioning booster seats and reduction in risk of injury in motor vehicles. JAMA Vol. 289, No. 10, pp 2835-2840, 2003.

Foster JK, Kortge JO, Wolanin MJ. Hybrid III – a biomechanically based crash test dummy. In Proc of the 21st Stapp Car Crash Conference, 1977.

Elhagediab AM, Hardy WN, Rouhana SW, Kent RW, Argoast KB, Higuchi K. Development of an instrumented rate-sensitive abdomen for the six year old Hybrid III dummy. JSAE Annual Congress Paper # 20075425, 2007.

Haut RC, Viano DC, Vostal JJ. Evaluation of the in vivo response to traumatic posterior tibia drawer. In Trans 26th Ann Meet Orth Res Soc, Atlanta, GA, 1980.

Hodgson VR, Thomas LM. Comparison of head acceleration injury indices in cadaver skull fracture. In Proc of 15th Stapp Car Crash Conference, 1971.

Howard A, Rothman L, McKeag A et al. Children in side impact motor vehicle crashes: seating positions and injury mechanisms. J Trauma Vol. 56, pp 1276-1285, 2003.

Hubbard RP. Flexure of layered cranial bone, J Biomech Vol 4, pp 251-263, 1971.

Irwin A, Mertz HJ. Biomechanical basis for the CRABI and Hybrid III child dummies. Society of Automotive Engineers Transactions. SAE Paper No. 973317, 1997.

Lopez-Valdes FJ, Forman J, Kent RW, Bostrom O, Segui-Gomez M. A comparison between a child-size PMHS and the Hybrid III 6 YO in a sled frontal impact. Ann Proc Assoc Automot Med Vol 53, pp 237-246, 2009.

Lopez-Valdes FJ, Lau A, Lamp J, Riley P, Lessley D, Damon A, Kindig M, Kent R, Balasubramanian S, Seacrist T, Maltese MR, Arbogast KB, Higuchi K, Tanji H. Analysis of spinal motion during frontal impacts. Comparison between PMHS and ATD. Ann Proc Assoc Automot Med *Accepted*.

McPherson GK, Kriewall TJ. The Elastic Modulus of fetal cranial bone: a first step towards an

understanding of the biomechanics of fetal head modeling. J Biomech Vol. 13, pp 9-16, 1981.

Menon R, Ghati Y, Ridella S, Roberts D, Winston F. Evaluation of Restraint Type and Performance Tested with 3- and 6-Year-Old Hybrid III Dummies at a Range of Speeds. SAE Paper No. 01-0319, 2004.

Menon RA, Ghati YS, Roberts D. Performance evaluation of various high back booster seats tested at 56 kph using a 6-year-old hybrid III dummy. In: Proceedings of the 19th International Technical Conference on the Enhanced Safety of Vehicles. Paper Number 05-0366. National Highway Traffic Safety Administration, Washington, DC, 2005.

Orzechowski K, Edgerton E, Bulas D, et al. Patterns of injury to restrained children in side impact motor vehicle crashes: the side impact syndrome. J Trauma Vol. 54, pp 1094-1101, 2003.

Panjabi MM, Cholewicki J, Nibu K, Babat L, Dvorak J. Simulation of whiplash trauma using whole cervical spine specimens. Spine Vol 23, pp 17-24, 1998.

Reed MP, Ebert-Hamilton SM, Schneider LW. Development of ATD installation procedures based on rear-seat occupant postures. Proc. 49th Stapp Car Crash Conference. Society of Automotive Engineers, Warrendale, PA.

Reed MP, Sochor MM, Rupp JD, Klinich KD, Manary MA. Anthropometric specification of child crash dummy pelves through statistical analysis of skeletal geometry. J Biomech Vol 42, pp 1143-1145, 2009.

Rouhana SW, Elhagediab AM, Walbridge A, Hardy WN, Schneider LW. Development of a Reusable, Rate-Sensitive Abdomen for the Hybrid III Family of Dummies. Stapp Car Crash J Vol 45, pp 33-60, 2001.

Shaw G, Parent D, Purtsezov S, Lessley D, Crandall J, Kent RW, Guillemot H, Ridella SA, Takhounts E, Martin P. Impact response of restrained PMHS in frontal sled tests: skeletal deformation patterns under seat belt loading. Stapp Car Crash J Vol 53, pp 1-48, 2009.

Sherwood CP, Shaw CG, van Rooij L, Kent RW, Gupta PK, Crandall JR, Orzechowski KM, Eichelberger MR, Kallieris D. Prediction of cervical spine injury risk for the 6-year-old child in frontal crashes. Ann Proc Assoc Adv Automot Med Vol 46, pp 231-247, 2002.

Thompson M, Irby J. Recovery from mild head injury in pediatric populations. Seminars in Pediatric Neurology Vol. 10, No. 2, pp 130-139, 2003.

Viano DC, Culver CC, Haut RC. The development of a model for the study of head injury. In Proc of 11th Stapp Car Crash Conference, 1978.

Wismans J, Van Oorschot H, Woltring H. Head-neck response to frontal flexion. In Proc. of the 30th Stapp Car Crash Conference, 1984.